Anal. Chem. **2001,** *73,* 870−877

2D Electrochemical Time of Flight and Its Application in the Measurements of the Kinetics of Lateral Electron Hopping in Monolayer Films at the Air/Water Interface

Michael Wittek, Gunter Möller, Michael J. Johnson, and Marcin Majda*

Department of Chemistry, University of California at Berkeley, Berkeley, California 94720-1460

A 2D electrochemical time-of-flight (ETOF) method was developed to measure diffusion constants of lateral mobility of amphiphiles and lateral electron hopping in Langmuir monolayers at the air/water interface. Photolithographically fabricated generator−collector ETOF devices featured two parallel gold microelectrodes (7 mm in length, 40 μm wide, spaced by a 10-μm gap). In 2D ETOF measurements, such a device is touching the water surface where the generator and collector electrodes function as a collinear pair of line microelectrodes. Bulk measurements, with a generator−collector device submerged in an electrolyte solution, were carried out to calibrate the devices by relating the transit times to the known *D* values of $Ru(NH_3)_6^{2+}$ in a series of solutions of different viscosity adjusted with sucrose. A new method to define and to measure transit times in the step mode ETOF experiments was developed that requires only the pseudo-steady-state values of the collector current. Reliability of the 2D ETOF technique was established by investigating lateral diffusion of an amphiphilic tetradecane TEMPO derivative for which the *D* values were also measured by 2D voltammetry. Combination of 2D ETOF and 2D voltammetry allows one to independently measure diffusion coefficients and concentrations of redox species. This advantageous feature was then used to reevaluate kinetics of lateral electron hopping in $Os(DPP)_3(ClO_4)_2$ (DPP, 4,7-diphenyl-1,10-phenanthroline) solid monolayers on the water surface. The true rate constant of electron self-exchange, $k_{ex} = 1.0 \times 10^9$ M^{-1} s^{-1}, was obtained. The fact that the latter is more than 1 order of magnitude larger than its value obtained in a homogeneous acetonitrile solution suggests that the structure and locale of the $Os(DPP)_3^{III+/II+}$ monolayer system result in a larger electronic coupling and/or smaller reorganization energy.

Lateral transport in Langmuir monolayers at the air/water interface encompasses a number of phenomena such as diffusion of lipids, their counterions, lateral electron hopping, and vectorial proton transport. The kinetics of these processes, which are of considerable importance to biomembrane science, are strongly affected by the composition, structure, and dynamics of the monolayer films as well as by the dynamic properties of the water liquid/vapor interfacial region. Lateral mobility of lipids in Langmuir films has been investigated by fluorescence photobleaching-photorecovery technique (FRAP).[1,2] FRAP and 2D voltammetric techniques with "line" microelectrodes[3] are analogous in that in both cases a gradient of a probe concentration in the plane of a Langmuir monolayer is established at the beginning of an experiment. Signal due to lateral diffusion of a labeled lipid is then followed as a function of time. The 2D voltammetric techniques are more general because they also allow investigations of the lateral electron[4] and proton[5] transport processes in addition to the measurements of the lipid lateral diffusion.[6] The line microelectrodes used in these techniques were specifically designed to be located (by self-positioning) directly in the plane of the air/water interface.[7] In this report, we describe a 2D electrochemical time-of-flight technique which offers some distinct advantages relative to 2D voltammetry.

An electrochemical time-of-flight (ETOF) experiment was first introduced by Murray and co-workers to investigate rates of electron propagation in polymer films.[8] Additional experimental aspects of the technique were further developed by Wrighton and co-workers and used to measure rates of diffusion of ions in polymeric and fluid solution media.[9−12] Theoretical modeling was done by Bard, Wrighton, and others.[13,14] ETOF is a transient

* Corresponding author: (e-mail) majda@socrates.berkeley.edu; (fax) (510) 643-1255.

(1) Peters, R.; Beck, K. *Proc. Natl. Acad. Sci. U.S.A.* **1983**, *80*, 7183−7187.
(2) Tamada, K.; Kim, S. H.; Yu, H. *Langmuir* **1993**, *9*, 1545−1550.
(3) Majda, M. Translational Diffusion and Electron Hopping in Monolayers at the Air/Water Interface. In *Organic Thin Films and Surfaces*; Ulman, A., Ed.; Academic Press: San Diego, 1995; Vol. 20, pp 331−347.
(4) Lee, W.-Y.; Majda, M.; Brezesinski, G.; Wittek, M.; Moebius, D. *J. Phys. Chem. B* **1999**, *103*, 6950−6956.
(5) Slowinska, K.; Majda, M., unpublished result, 2000.
(6) Kang, Y.-S.; Majda, M. *J. Phys. Chem. B* **2000**, *104*, 2082−2089.
(7) Charych, D. H.; Landau, E. M.; Majda, M. *J. Am. Chem. Soc.* **1991**, *113*, 3340−3346.
(8) Feldman, B. J.; Feldberg, S. W.; Murray, R. W. *J. Phys. Chem.* **1987**, *91*, 6558−6560.
(9) Licht, S.; Cammarata, V.; Wrighton, M. S. *Science* **1989**, *243*, 1176−1178.
(10) Cammarata, V.; Talham, D. R.; Crooks, R. M.; Wrighton, M. S. *J. Phys. Chem.* **1990**, *94*, 2680−2684.
(11) Licht, S.; Cammarata, V.; Wrighton, M. S. *J. Phys. Chem.* **1990**, *94*, 6133−6140.
(12) Tatistcheff, H. B.; Fritsch-Faules, I.; Wrighton, M. S. *J. Phys. Chem.* **1993**, *97*, 2732−2739.
(13) Bard, A. J.; Crayston, J. A.; Kittlesen, G. P.; Shea, T. V.; Wrighton, M. S. *Anal. Chem.* **1986**, *58*, 2321−2331.

10.1021/ac001015i CCC: $20.00
Published on Web 02/02/2001

generator−collector-type technique involving a pair or an array of narrowly spaced microelectrodes operated under controlled potential conditions in a bipotentiostatic circuit. One of the electrodes (or a half of an interdigitated array of microelectrodes) functions as a generator. An experiment is initiated by applying a potential pulse or a step (pulse or step mode) to that electrode to electrogenerate redox species that then begin to diffuse and are "collected" at the other microelectrode, which is held at a constant potential selected to allow the reverse of the generator redox reaction to take place. Thus, the measurements involve recording of the collector current transients ($i_{col} - t$) which are then used to determine transit times (τ). The latter are proportional to the inverse of the diffusion coefficient (D) of the electrogenerated redox species and the square of the distance between the generator and collector electrodes (d):[8,11]

$$\tau = \mathrm{K}d^2/D \qquad (1)$$

The constant factor K depends on the geometry of a generator−collector device, on the mode of the experiment (pulse or step), and on the specific definition of transit time. Calibration curves (τ vs $1/D$) must be obtained by carrying out ETOF experiments with species of known D values.

One crucial advantage of the ETOF technique, which we exploit in this report, is the ability to yield D values without requiring the concentration of the redox species as an input parameter (see eq 1). This is contrary to the voltammetric techniques in which measured current is related to both diffusion constant and concentration of the redox species.[15] Monolayers formed on the water surface often exhibit nonhomogeneous morphologies resulting in differences in a local surface concentration. Also, the degree of electrochemical activity of the redox molecules in such structurally heterogeneous films may be uncertain. Consequently, when lateral diffusion processes are probed with 2D voltammetry, the use of an apparent (average) surface concentration to interpret measured current introduces an uncertainty in the resulting D values. An example of this type of case is osmium tris-4,7-diphenyl-1,10-phenanthroline perchlorate ($Os(DPP)_3$) which forms monolayers consisting of 2D solid, irregularly shaped aggregates varying in size from about 100 to 1000 μm in diameter.[4] Brewster angle microscopy revealed that slow compression of these aggregates results, ultimately, in their coalescence and formation of a macroscopically homogeneous monolayer.[4,16] Below, we describe the development of a 2D electrochemical time-of-flight technique. We first show that, in the case of liquid monolayers of a tetradecane TEMPO-amide amphiphile (C_{14}TEMPO), 2D voltammetry and ETOF give the same values of the lateral diffusion constant. We then use 2D ETOF to investigate rates of diffusive lateral electron hopping in $Os(DPP)_3$ monolayers at the air/water interface and compare these measurements with the earlier data obtained by 2D voltammetry.

EXPERIMENTAL SECTION

Reagents. The syntheses of $Os(DPP)_3$[17] and 4-tetradecaneamido-2,2,6,6-tetramethyl-1-piperidinyloxy (C_{14}TEMPO)[18] were carried out according to the procedures described previously. House-distilled H_2O was passed through a three-cartridge Millipore purification train consisting of a Macropure pretreatment, an Organics Free cartridge for removal of trace organic contaminants, an ion exchanger, and a 0.2-μm hollow-fiber final filter for removing particles. The resistivity of the resulting water (DI water) was >18.3 MΩ cm. Octadecyltrichlorosilane (OTS) and 3-mercaptopropyltrimethoxysilane (MPS) were from Aldrich. OTS was vacuum-distilled into sealed glass ampules, which were opened as needed immediately prior to the individual experiments. Octadecylmercaptan (OM) (Tokyo Kasei, Tokyo, Japan) was used without further purification. Reagent grade 70% $HClO_4$ (Fisher, ACS certified), chloroform (Fisher, ACS certified spectranalyzed), methanol (Fisher, spectroscopic grade), and all the other reagents are used as received.

Monolayer Techniques. Experiments at the air/water interface were carried out in a 10 × 20 cm^2 home-built Teflon trough equipped with a mechanically driven barrier (under computer control) and a Wilhelmy plate-type surface pressure microbalance. Filter paper was used to prepare Wilhelmy plates. A commercial Langmuir trough instrument (KSV model 2200) was used to record $\pi-A$ isotherms and Brewster angle micrographs. All experiments involving Langmuir troughs were done in an inert gas plexiglass enclosure. $Os(DPP)_3$ monolayers were spread on a 50 mM perchloric acid subphase from 0.133 mM chloroform solutions at an initial area of 360 Å^2/molecule and compressed at a rate of 13 Å^2/molecule per minute. The C_{14}TEMPO monolayers were spread from 1.0 mM chloroform solutions at 120 Å^2/molecule and compressed also at 13 Å^2/molecule per minute.

Fabrication of the Generator−Collector Microband Devices. The design of these devices features three, parallel 40-μm-wide microband electrodes separated by 10-μm gaps. A schematic drawing of the design is shown in Figure 1. Since the same devices are to be used both in the 3D (bulk mode) experiments and in the 2D ETOF experiments at the air/water interface, the tips of the three microbands must coincide with the edge of a glass substrate. To accomplish this, the pattern shown in Figure 1 features a pair of such devices positioned as a mirror image of each other. Following their fabrication, individual devices are produced by fracturing glass slides along the dashed line shown in the figure. Each of the three 7-mm-long microbands can be independently addressed via a 4 × 6 mm^2 contact pad. While the use of three electrode devices (a generator flanked by two collector electrodes) offers a higher collection efficiency,[13] only two adjacent microbands were used in our ETOF experiments. This improved the success rate of obtaining a working device which we found more advantageous than a somewhat higher current sensitivity of the three-electrode ETOF devices.

Glass slides (Corning 2947) used as substrates were first cleaned in a hot chromic acid solution for ~60 min., repeatedly rinsed with DI water, and dried under nitrogen. Next, they were treated with MPS to provide adequate adhesion for the subse-

(14) Fosset, B.; Amatore, C.; Bartlet, J.; Wightman, R. M. *Anal. Chem.* **1991**, *63*, 1403−1408.
(15) Galus, Z. *Fundamentals of Electrochemical Analysis*, 2nd ed.(revised); Ellis Horwood Limited: Chichester, 1994; Chapter 6.1, p 141.
(16) Charych, D. H.; Anvar, D. J.; Majda, M. *Thin Solid Films* **1994**, *242*, 1−6.
(17) Gaudiello, J. G.; Bradley, P. G.; Norton, K. A.; Woodruff, W. H.; Bard, A. J. *Inorg. Chem.* **1984**, *23*, 3.
(18) Rozantsev, E. G.; Suskina, W. I. *Akad. Nauk SSSR: Izvest.: Ser. Khim.* **1969**, *5*, 1191−1193.

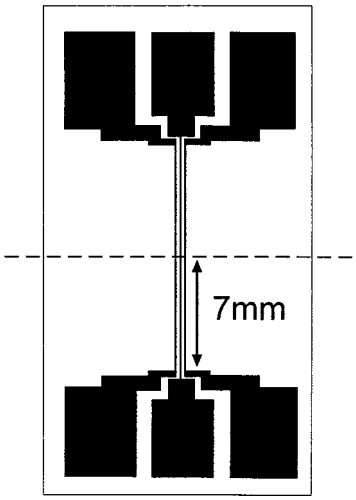

Figure 1. Schematic drawing of the collector−generator device. The microband electrodes are 40 μm wide and are spaced by 10-μm gaps. In collector−generator ETOF experiments, only one of the two side microelectrodes was used.

quently vapor-deposited gold layer. The MPS treatment (a modification of our earlier procedure)[19] involved immersion of the glass slides into a 2% MPS solution in trichloroethylene (TCE) under nitrogen for 3−4 h. Subsequently, the slides were rinsed sequentially with TCE, acetone, 2-propanol, and DI water and dried under a stream of nitrogen. They were then baked for ∼10 min at 105−110 °C in a drying oven. Vapor deposition of a 800-Å-thick gold film followed at $\sim 5 \times 10^{-7}$ Torr. The gold-coated glass slides were then used to fabricate the three-electrode devices described above using a standard, photolithographic procedure with a wet gold etching. The mask and the devices were produced in the UCB Microfabrication Laboratory.

Fabrication of the Devices for the 2D ETOF. The 2D electrochemical measurements at the air/water interface require generator−collector devices that can be positioned and function in the plane of the air/water interface as "line" microelectrodes (see Figure 2). These types of microelectrodes are produced by creating a sharp gradient of wettability along a fracture line of a patterned, microfabricated gold film.[7] This involves self-assembly of the OM and OTS monolayers on the microfabricated gold and on glass surfaces, respectively. This renders all the surfaces of the substrate hydrophobic. By breaking such an electrode substrate in half (along a line drawn with a diamond pencil on the reverse side of the glass substrate shown with a dashed line in Figure 1), one exposes a clean, and thus hydrophilic, edge surface of glass and gold and creates two identical microelectrode devices. The newly exposed edges of gold form 40-μm-long microband electrodes.

The microelectrode devices are positioned at the air/water interface by touching the water surface with the clean, hydrophilic edge of the electrode substrate. The line of wettability that is formed spontaneously along the edge of the gold microband between the hydrophilic gold cross-sectional area and the hydrophobic (OM-coated) front face of the gold strip functions as a line electrode. Thus, simple wetting of the gold microband results in self-positioning of the line electrode in the plane of the water surface. The electrodes were always positioned at the air/water interface following monolayer spreading and solvent evaporation. At the air/water interface, their performance is reproducible for ∼10−20 min. Later their performance begins to deteriorate due to adsorption of impurities.

Electrochemical Experiments. The D values for $Ru(NH_3)_6^{3+}$ were measured using a PAR model 303A (EG&G Ins.) static mercury drop electrode in hanging mode using cyclic voltammetry. The 2D ETOF and voltammetry were performed with an Ensman model 852 bipotentiostat (Bloomington, IN) in a four- and three-electrode configuration, respectively, under computer control. The reference electrode (SCE) and counter (Pt) electrodes were immersed in the subphase in a Langmuir trough behind the barrier in order not to disturb Langmuir monolayers. Before each 2D ETOF experiment, 2D voltammograms were recorded on each of the two microband electrodes to ensure that each was well behaved. Those devices showing excessive capacitive current (>0.5 nA) or other signs of malfunctioning were discarded.

Calibration of the generator−collector devices was done in 5 mM $Ru(NH_3)_6^{3+}$ (Strem Chemicals), 0.1 M KCl (Fisher Scientific ACS grade) solutions made to contain specific amounts of sucrose (Aldrich, ACS grade) used to increase their viscosity. The D values for $Ru(NH_3)_6^{2+}$ in these solutions were obtained using a literature value of $D_{Ru(NH_3)_6^{2+}}$ in water[11] and correcting it by the average ratio of the voltammetric peak currents recorded in the standard $Ru(NH_3)_6^{3+}$ solution containing no sucrose and in those containing variable sucrose concentrations. The precision of the method based on at least four independent experiments with different Hg drop electrodes was 2−3%.

RESULTS AND DISCUSSION

2D vs 3D ETOF Experiments. 2D electrochemical time-of-flight measurements involve microfabricated devices with two parallel microband electrodes vapor-deposited on glass slides (see Figure 1 and the Experimental Section for details of the fabrication and chemical treatment of such devices). These devices can be used both in the 3D- and 2D-type ETOF experiments. In the latter case, the edges of the two electrodes are touching the water surface as shown in Figure 2. The sharp gradient of wettability between the cross-sectional areas of the vapor-deposited gold film (40×0.1 μm^2, created by fracturing the originally produced electrode substrates) and the OM-treated face surfaces of the gold deposit is the crucial feature of the design. It allows the edges of the two microband electrodes to be located exactly in the plane of the air/water interface and thus to function as line microelectrodes.[7] The essential dimensions of the device (width of each microband, $w = 40$ μm, interelectrode gap, $G = 10$ μm, length of the microbands, $l = 8$ mm) were optimized by taking into consideration the collector current sensitivity and a capacitive coupling (cross-talk) between the generator and collector electrodes resulting in a characteristic collector current spike at $t = 0$. Both of these decrease with increasing G. We found that the capacitive coupling spikes interfered excessively with the leading edge of the collector current transients when devices with $G < 5$ μm were used.

As shown schematically in Figure 3, both 3D- and 2D-type ETOF experiments generate analogous shapes of the concentration profiles. For example, in the early stages of an experiment

(19) Goss, C. A.; Charych, D. H.; Majda, M. *Anal. Chem.* **1991**, *63*, 83−88.

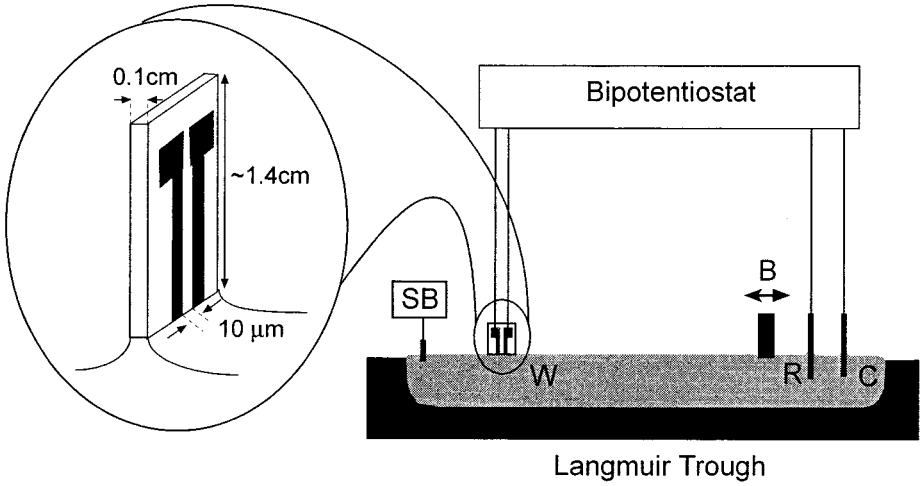

Figure 2. Schematic diagram of an experimental setup used to record $\pi-A$ isotherms, Brewster angle micrographs (BAM) and 2D ETOF data. Key: B, movable barrier of the Langmuir trough; C, counter electrode; R, reference electrode; W, working collector−generator microelectrode device, SB, surface film balance. The inset shows the position of the collector−generator line microelectrodes (shown in Figure 1) at the water surface.

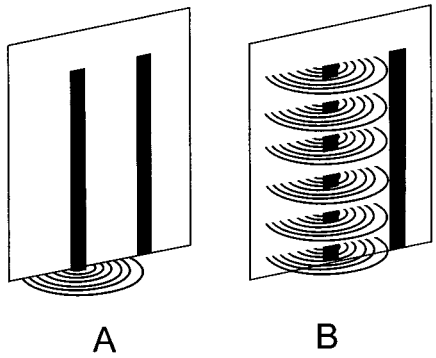

Figure 3. Schematic drawing of the hemicircular (A) and hemicylindrical (B) diffusion patterns developing during an initial stage of an ETOF experiment at the generator microelectrode functioning either as a line microelectrode in the plane of the air/water interface (A) or as a microband electrode submerged in an electrolyte solution (B).

depicted in Figure 3, a hemicylindrical diffusion governs mass transport of the electrogenerated species in the 3D (bulk) case, and an analogous, hemicircular diffusion is involved in the 2D case. In an earlier report, we quantitatively demonstrated that hemicircular diffusion in 2D and hemicylindrical diffusion in 3D systems are equivalent.[20] This is to say that the time evolution of fluxes in a 2D system at the line electrode (with length w) and at a microband electrode (with length l and width w) in a 3D solution follows the same equations except that the change of dimensionality from 3D to 2D converts the product $l \times C^*$ into Γ^*, preserving its units (mol/cm^2). C^* and Γ^* represent the bulk solution and monolayer concentrations of the electroactive species, respectively. For example, it is well known that in the case of a single microband electrode for sufficiently long times such that $Dt/w^2 > 1$, chronoamperometric current can be expressed by[21,22]

$$i = \frac{2\pi nFDlC^*}{\ln(64Dt/w^2)} \qquad (2)$$

The equivalent current in a 2D chronoamperometric experiment done with a line electrode with length w (equal to the width of the microband in the 3D case) is expressed by[20]

$$i = \frac{2\pi nFD\Gamma^*}{\ln(64Dt/w^2)} \qquad (3)$$

In view of the above, while the steady-state shape of the concentration profiles developing between the generator and collector electrodes during an ETOF experiment are different from those in Figure 3,[23] we can rely on the 3D calibration experiments described below and use their results to interpret 2D ETOF transients.

ETOF Transit Times and the Calibration Protocol. Interpretation of collector current transit times (τ, see eq 1 above) requires a calibration curve constructed on the basis of a set of experiments involving electroactive species with known diffusion constants. These experiments were done with the generator−collector microband electrodes submerged in the $Ru(NH_3)_6^{3+}$ solutions containing different concentrations of sucrose. To maximize collector current in the subsequent 2D ETOF measurements, potential steps rather than short pulses were used to generated electroactive species. Wrighton and co-workers estimated that this so-called potential step mode gives an order of magnitude increase in collector current sensitivity relative to the pulse mode ETOF experiments in which a short potential pulse is applied to the generator electrode.[11] In the latter case, reversing the generator potential to its initial value at the end of the pulse results in reconversion of the electrogenerated species, a process that drastically reduces the flux of the latter to the collector electrode and results in the peak-shaped collector currents.[8,11] In contrast, in step mode ETOF experiments, the potential applied to the generator electrode is held for a sufficiently long time to

(20) Charych, D. H.; Goss, C. A.; Majda, M. *J. Electroanal. Chem.* **1992**, *323*, 339−345.

(21) Galus, Z. *Fundamentals of Electrochemical Analysis*, 2nd ed. (revised); Ellis Horwood Limited: Chichester, 1994; Chapter 6.3, p 206.

(22) Szabo, A.; Cope, D. K.; Tallman, D. E.; Kovach, P. M.; Wightman, R. M. *J. Electroanal. Chem.* **1987**, *217*, 417−423.

(23) Fosset, B.; Amatore, C. A.; Bartelt, J. E.; Michael, A. C.; Wightman, R. M. *Anal. Chem.* **1991**, *63*, 306−314.

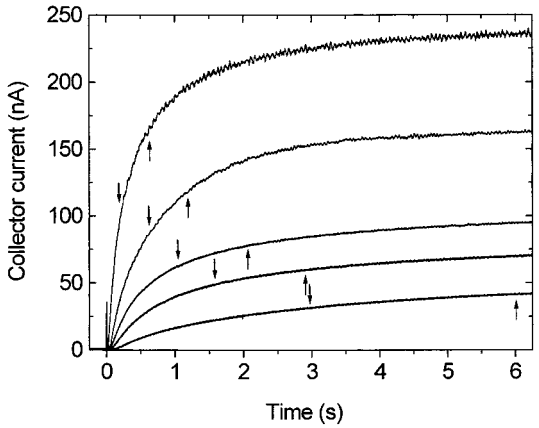

Figure 4. A set of five collector current transients recorded at 0.0 V in 5 mM $Ru(NH_3)_6^{3+}$, 0.1 M KCl solution containing (top to bottom) 0, 20, 34, 40, and 48 wt % sucrose. The collector−generator devices were immersed in these solutions to a depth of ~5 mm. The transients were recorded after the potential of the generator electrode was stepped from 0.0 to −0.4 V at $t = 0$. The values of the pseudo-steady-state times (t_{pss}) for the transient recorded in the 48 wt % sucrose solutions were arbitrarily selected to be 3 (down-pointing arrow) and 6 s (up-pointing arrow). The remaining up- and down-pointing arrows mark the positions of the equivalent t_{pss} values calculated according to eq 5.

allow steady-state conditions to develop.[11,14,23] Due to the feedback effect existing between the collector and generator electrodes,[11] the steady-state collector current is substantially greater than the peak current observed at the collector electrode in the pulse mode experiments.

A set of step mode collector current transients due to reoxidation of electrogenerated $Ru(NH_3)_6^{2+}$ is shown in Figure 4. The five transients were recorded in 5.0 mM $Ru(NH_3)_6^{3+}$ solutions containing between 0 and 48 wt % sucrose. The latter was used to increase solution viscosity and thus to cover a range of $D_{Ru(NH_3)_6^{2+}}$ values from 7.8×10^{-6} to 6.2×10^{-7} cm^2/s. The values of $D_{Ru(NH_3)_6^{2+}}$ in these solutions were measured voltammetrically at a hanging mercury drop electrode (see Experimental Section).

In the step mode ETOF experiments, transit time (τ) can be defined as a time required for a collector current to reach a certain arbitrarily chosen fraction of its maximum plateau value. However, the collector current approaches its steady-state plateau value slowly.[14,23] This effect is further exacerbated in cases involving species with low diffusion coefficients**.** In Figure 4, the collector current in the experiment done with 0 wt % sucrose reaches its plateau value after ~8 s. In the more viscous solutions, the collector current transients require, naturally, considerably longer times to reach their maximum values. In those cases, the signal-to-noise ratio deteriorates considerably due to convective fluctuations and makes recording of the plateau currents inaccurate and simply impractical. To circumvent these difficulties, we developed a method that does not require knowledge of the true, steady-state collector currents. It is based on a simple premise (see eq 1) that the transit times of two species of different diffusion constants (D_1 and D_2) obtained with the same device are related by the inverse ratio of their D values:

$$\tau(1) = \tau(2)(D_2/D_1) \qquad (4)$$

Consequently, the times required to achieve the true steady-state

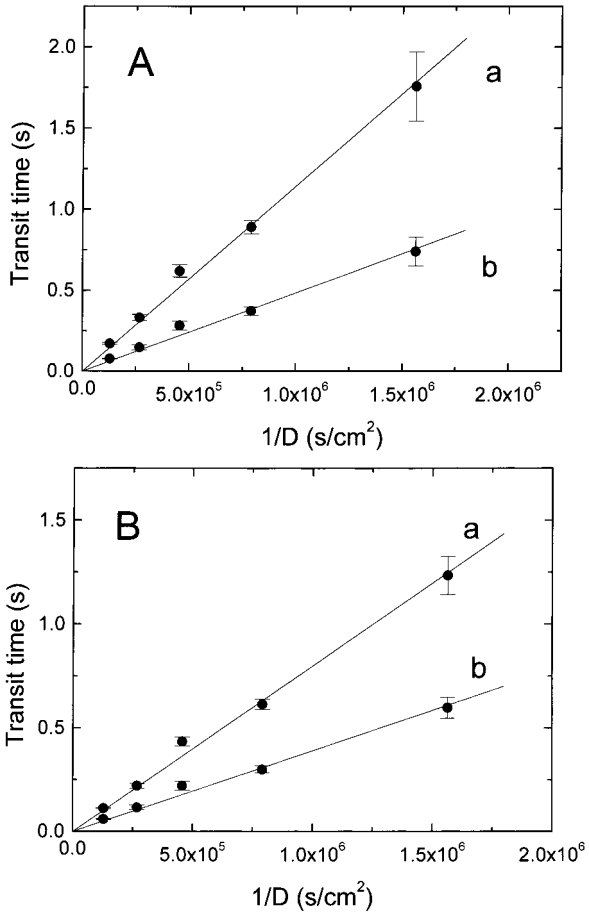

Figure 5. Four equivalent calibration curves (τ vs $1/D$) obtained on the basis of the data in Figure 4. They differ by the values of the initial (48 wt % sucrose) pseudo-steady-state time (t_{pss}) (A, t_{pss}= 6 s; B, t_{pss}= 3 s), and by the selection of a fraction of the collector current at the equivalent t_{pss} to be reached at t (a, 60%; b, 30%).

current must also be likewise related. Accordingly, we first arbitrarily select a time (typically 3−6 s) referred to as pseudo-steady-state time (t_{pss}). At this time, the collector current corresponding to the slowest diffusing species (obtained in the most viscous sucrose solution of 48 wt %) reached only a certain small fraction of its true steady-state value. Next, we calculate the equivalent t_{pss} values for the other transients. In view of eq 4, in all the cases of less concentrated sucrose solutions, the same fraction of the true steady-state current was reached more rapidly (at a shorter t_{pss}) by a factor equal to the ratio of the known $Ru(NH_3)_6^{2+}$ diffusion constants in the most viscous solution and that in a given solution. For example, for a 20 wt % sucrose solution

$$t_{pss}(20\%) = t_{pss}(48\%)D_{48\%}/D_{20\%} \qquad (5)$$

where $D_{48\%}$ and $D_{20\%}$ stand for the $Ru(NH_3)_6^{2+}$ diffusion constants measured in the solutions containing the subscripted level of sucrose. The calculated equivalent t_{pss} values for all the transients are marked in Figure 4. The collector currents at the equivalent t_{pss}'s are then used as reference values to obtain transit times (τ). Those were defined as the time required for the collector current to reach either 30 or 60% of the reference values at those points. As shown in Figure 5, selection of neither a t_{pss} value for the

transient recorded in the most viscous sucrose solution nor the current fraction (30 vs 60%) affects the linearity of the calibration plots (τ vs $1/D$). Naturally, in order to use one of these calibration plots in the interpretation of the 2D or 3D collector current transients due to species of an unknown diffusion constant, the same t_{pss} and current fraction must be used. To obtain the equivalent t_{pss} value, one begins with a guess of a seed value, $D(1)$, and calculates $t_{pss}(1)$ using any of the known t_{pss} values from the calibration experiments. For example

$$t_{pss}(1) = t_{pss}(48\%)D_{48\%}/D(1) \qquad (6)$$

Subsequently, $t_{pss}(1)$ is used to obtain $\tau(1)$ and then $D(2)$ from the calibration curve. This iterative protocol is then repeated until $t_{pss}(n) = t_{pss}(n-1)$ and $D(n) = D(n-1)$.

Lateral Diffusion of C_{14}TEMPO at the Air/Water Interface. The chemical structure of C_{14}TEMPO, an electrochemically active lipid is shown in Figure 6A. A full description of the electrochemical behavior and surface properties of C_{14}TEMPO is the subject of a separate report.[24] Here we use it as an example of a well-behaved, fluid monolayer system. Specifically, $\pi-A$ diagrams and Brewster angle microscopy showed that Langmuir films of C_{14}-TEMPO are homogeneous in a broad range of surface concentrations.[24] The lateral mobility of C_{14}TEMPO obtained by 2D voltammetry increases linearly with the mean molecular area in a range from 60 to ~150 Å^2/molecule.[24] This is consistent with the expected increase of a monolayer fluidity upon its expansion.[1,6] The lateral diffusion constants of C_{14}TEMPO were remeasured using 2D voltammetry and the 2D ETOF technique. Measurements using these two techniques were done sequentially with one (2D voltammetry) or both (2D ETOF) microband electrodes of a given collector-generator device. A typical 2D voltammogram and a collector current transient are shown in Figure 6. The shape of the voltammogram in Figure 6A reveals the presence of a radial component. This is not surprising in this case since the diffusion layer thickness (approximated by $(2Dt)^{1/2}$) is ~20 μm under the experimental conditions of Figure 6A, a value comparable to the length of the line electrode of 40 μm. Consequently, to obtain the D values, the 2D voltammetric peak currents were interpreted in terms of the methodology developed by Aoki and co-workers.[25] It is interesting to point out that the interpretation of the 2D ETOF transients such as that in Figure 6B yields a diffusion constant of the oxidized form of C_{14}TEMPO. We showed recently that the lateral mobilities of amphiphiles on the water surface are governed predominantly by their immersion depth, which depends in turn on the extent of charging and/or polarity of their headgroups. Since complete ion-pairing of $C_{14}TEMPO^+$ with NO_3^- ions (available in the 50 mM HNO_3 subphase) can be deduced from the insolubility of the oxidized form, we can assume that the D values of both oxidation states are nearly identical.

In view of the well-behaved, single-phase character of the C_{14}-TEMPO monolayers mentioned above,[24] we expected the average and microscopic surface concentrations of C_{14}TEMPO to be the same. Thus, determination of D values by 2D ETOF and 2D

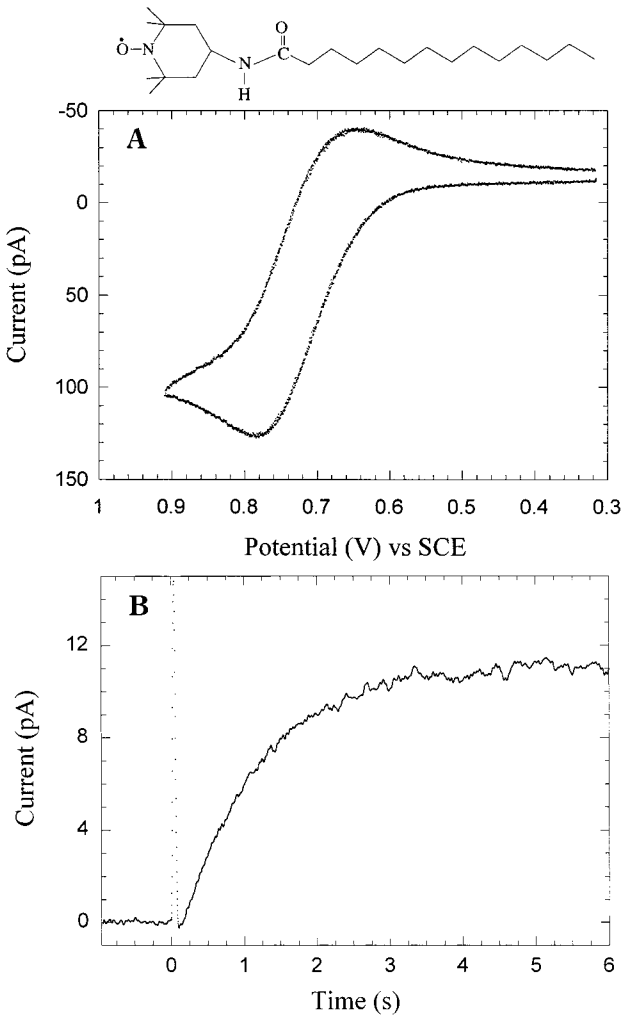

Figure 6. 2D voltammetry (A) and 2D ETOF transient (B) of a C_{14}-TEMPO monolayer at 60 Å/molecule (chemical structure is shown in frame A) at the air/water interface (50 mM HNO_3) recorded with a generator−collector line microelectrode device positioned in the plane of the water surface as shown in Figure 2. A, scan rate 0.2 V/s; B, the collector electrode was held at 0.3 V while the potential of the generator electrode was stepped from 0.3 to 0.9 V at $t = 0$. The sharp current spike at $t = 0$ is a result of a capacitive cross-talk between the generator and collector electrodes.

voltammetry should yield the same results. This is indeed seen in Figure 7. These results support our assertion that the bulk mode (3D) calibration of the ETOF devices is valid in the 2D experiments.

2D Diffusive Electron Hopping in $Os(DPP)_3$ Monolayers on the Water Surface. $Os(DPP)_3$ forms solid 2D aggregates when spread on the water surface (50 mM $HClO_4$). The morphology and structure of the $Os(DPP)_3$ monolayers were characterized using Brewster angle microscopy and grazing incidence X-ray diffraction (GIXD).[4] These showed that the hexagonally close-packed structure of the osmium complex (with Os−Os distances of 12.57 Å) does not depend on the extent of monolayer compression. The latter results merely in macroscopic coalescence of the initially formed aggregates. Our earlier 2D voltammetric measurements showed that the lateral electron transport in Os-$(DPP)_3$ monolayers involved electron hopping on the 2D lattice of the osmium sites altering their oxidation state, Os(II)/Os(III). We invoked percolation theory to account for the observed

(24) Johnson, M. J.; Anvar, D. J.; Skolimowski, J. J.; Majda, M. *J. Phys. Chem. B.* **2001**, *105*, 514−518.
(25) Aoki, K.; Honda, K.; Tokuda, K.; Matsuda, H. *J. Electroanal. Chem.* **1985**, *182*, 267−279.

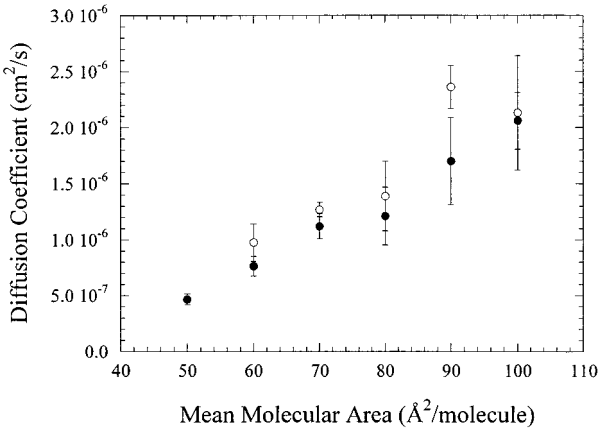

Figure 7. Comparison of the lateral diffusion coefficients of C_{14}-TEMPO in its monolayers at the air/water interface obtained by 2D voltammetry (closed circles) and 2D ETOF (open circles). The error bars represent standard deviations of typically three to five independent measurements.

increase in the apparent diffusion constant (D_{app}) of electron hopping during monolayer compression.[4] The latter reflected an increase of the extent of connectivity and thus electroactivity of the initially formed 2D $Os(DPP)_3$ aggregates. The maximum value of D_{app} of 8×10^{-7} ($\pm$15%) cm^2/s was obtained at 90 $Å^2$/molecule (corresponding to the average surface concentration of 1.84×10^{-10} mol/cm^2). That value of D_{app} was obtained from the 2D voltammetric peak currents under the assumption that the microscopic concentration of the osmium sites is equal to its apparent macroscopic value given above and that all the osmium sites are electroactive. However, high-resolution BAM images showed that at 90 $Å^2$/molecule the monolayer is not fully homogeneous and that there exist regions of partially collapsed morphology where overlap between adjacent aggregates could be seen. Assuming that the electron hopping involves only the 2D domains (with $Os(DDP)_3$ surface concentration of 1.21×10^{-10} mol/cm^2 obtained from the GIXD data), the 2D voltammetric current at a state of maximum compression was reinterpreted to yield $D_{app,cor} = 1.8 \times 10^{-6}$ cm^2/s. While that value was based on the microscopic Os−Os distances (12.57 Å), we could not be sure whether the $Os(DPP)_3$ monolayers were fully electroactive. We address this question now by measuring the D values of the lateral electron hopping using the 2D ETOF technique. As mentioned above, measurements of D values by 2D ETOF do not require surface concentration as an input parameter. The diffusion constants obtained this way (D_{ETOF}) are then used to calculate the electrochemically active surface concentration of the osmium complex from the 2D voltammograms.

The 2D voltammetric and ETOF experiments were carried out in the range of mean molecular areas of 80−120 $Å^2$/molecule. The former involved one of the 40-μm line electrodes of the ETOF devices described above and were done immediately prior to the time-of-flight measurements. Thus, both types of experiments involve the same fragment of an $Os(DPP)_3$ aggregate. A typical 2D voltammogram and a collector current transient are shown in Figures 8. As the monolayer was compressed, the voltammetric current increased and the transient times became shorter. Both of these trends reflected an increasing electroactivity of the $Os(DPP)_3$ monolayer and electron hopping percolation as discussed

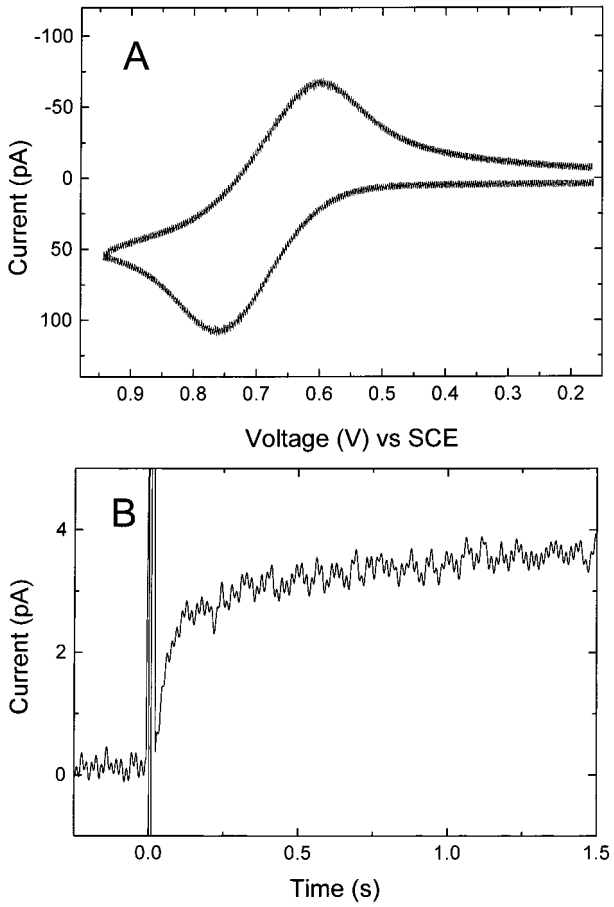

Figure 8. 2D voltammetry (A) and 2D ETOF transient (B) of a $Os(DPP)_3$ monolayer (at an apparent mean molecular area of 95 Å/molecule) at the air/water interface (50 mM $HClO_4$) recorded with a generator−collector line microelectrode device positioned in the plane of the water surface as shown in Figure 2. A, scan rate 0.2 V/s; B, the collector electrode was held at 0.2 V while the potential of the generator electrode was stepped from 0.2 to 0.95 V at $t = 0$. A sharp current spike induced by the potential step at the generator electrode is visible at $t = 0$.

previously.[4] Data recorded below 90 $Å^2$/molecule become irreproducible due to monolayer collapse. Both sets of 2D electrochemical measurements were then interpreted in terms of the lateral diffusion constant of electron hopping. The results are collected in Figure 9. To evaluate voltammetric peak currents, the apparent surface concentrations of $Os(DPP)_3$ were calculated from the mean molecular areas at which these 2D voltammograms were recorded. The 2D version of the voltammetric Randles−Ševčik equation[15] was used:

$$i_p = 2.69 \times 10^5 n^{3/2} D_{app}{}^{1/2} v^{1/2} w\Gamma^* \qquad (7)$$

Here again the product of surface area and bulk concentrations (AC^*) is replaced by the product of the electrode length and surface concentration of the electroactive species ($w\Gamma^*$). To interpret the collector current transients, the calibration curves in Figure 5 and the protocol described above were used.

Comparison of the two sets of D values in Figure 9 clearly suggests that the apparent concentrations of $Os(DPP)_3$ used in the interpretation of the 2D voltammograms are burdened with a

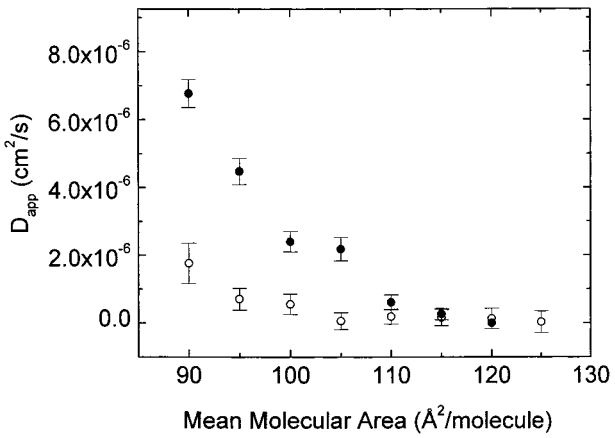

Figure 9. Dependence of the diffusion constant of the lateral electron hopping in the $Os(DPP)_3$ monolayers on the water surface (50 mM $HClO_4$) on the apparent mean molecular area of the osmium complex. The open circles correspond to the values obtained from the peak currents of 2D voltammograms such as that in Figure 8A using eq 7 and the apparent surface concentrations of the osmium sites. The closed circles represent data obtained from the 2D ETOF experiments. The error bars represent standard deviations of eight independent measurements.

large positive error. The maximum value of D (6.8×10^{-6} cm^2/s) obtained from the 2D ETOF measurements at 90 Å^2/molecule can be taken as the true value of the lateral electron hopping diffusion constant. When this value of D is used to interpret the voltammetric peak current recorded at 90 Å^2/molecule (corresponding to 1.8×10^{-10} mol/cm^2), the electrochemically active $Os(DPP)_3$ concentration, $\Gamma_{true} = 9.5 \times 10^{-11}$ mol/cm^2, is obtained. Clearly, this value is almost a factor of 2 smaller. This large discrepancy is due to a macroscopic disorder and partial collapse of the compressed $Os(DPP)_3$ monolayers mentioned above and discussed previously.[4] A more insightful comparison involves Γ_{true} and the $Os(DPP)_3$ surface concentration in the ordered domains calculated from the X-ray diffraction data, $\Gamma_{x-ray} = 1.2 \times 10^{-10}$ mol/cm^2. To discuss this comparison, we recall that the grazing angle X-ray diffraction analysis suggested that the ordered domains of the osmium complex were microcrystalline with the coherence length on the order of only ~100 Å.[4] Thus it appears that some loss of electroactivity suggested by a 27% smaller electroactive concentration of the osmium sites relative to its crystallographic concentration could be due to the inactivity of the sites at the grain boundaries.

Finally, the maximum value of D obtained by 2D ETOF together with the crystallographic Os−Os distance gave us a reliable assessment of the unimolecular (k_1) and the bimolecular (k_{ex}) rate constants of electron self-exchange. Using the approach described previously,[4] we obtained the following: $k_1 = 1.7 \times 10^9$ s^{-1} and $k_{ex} = 1.0 \times 10^9$ M^{-1} s^{-1}. The latter is more than 1 order of magnitude higher than a literature value obtained in an acetonitrile solution.[26] The rather substantial enhancement of the electron-transfer kinetics in a solid $Os(DPP)_3$ monolayer could be due to one or both of the following factors. (1) The distances between the osmium centers and a particular alignment of the DPP ligands could result in a higher electronic coupling between Os(II) and Os(III) relative to the those prevailing when these ions collide and exchange an electron in a homogeneous solution. (2) The reorganization energy of the $Os(DPP)_3$ molecules in a monolayer at the water surface could be smaller due to a partial solvation. Measurements of the reorganization energy directly at the air/water interface should provide more insight.

(26) Chan, M.-S.; Wahl, A. C. *J. Phys. Chem.* **1978**, *82*, 2542−2549.

CONCLUSIONS

We described the development of a 2D ETOF technique and demonstrated its usefulness in the investigations of the kinetics of lateral processes in Langmuir monolayer films. The key advantage of the ETOF technique is that it allows one to determine diffusion constants without knowledge of the concentration of the diffusing species. We took advantage of this capability of 2D ETOF to gain new insight into the dynamics of electron hopping in solid $Os(DPP)_3$ monolayers on the water surface. Combination of 2D ETOF and 2D voltammetry in these investigations allowed us to independently measure both the true electron hopping diffusion constant and the true surface concentration of the osmium sites. Comparison of the latter with the surface concentration obtained from our earlier X-ray diffraction data suggests that as much as 27% of the sites in the 2D domains are not electrochemically active due to their location at the grain boundaries. These measurements allowed us also to obtain the true rate constant of electron transfer between neighboring osmium sites in these 2D solid domains. The fact that this value is more than 1 order of magnitude larger than that obtained in a homogeneous solution provokes some additional questions concerning the strength of the electronic coupling and the magnitude of the reorganization energy of this redox couple. Independent determination of these parameters is contemplated and would further deepen our understanding of the electron-transfer dynamics in these unusual 2D solid monolayer aggregates.

ACKNOWLEDGMENT

Acknowledgment is made to the donors of the Petroleum Research Fund, administered by the ACS, for a partial support of this research. Additional support was provided by the National Science Foundation under Grant CHE-0079225. G.M. acknowledges his postdoctoral fellowship from Deutsche Forschungsgemeinschaft.

Received for review August 24, 2000. Accepted November 30, 2000.

AC001015I